The Relationship between Stress Fiber-Like Structures and Nascent Myofibrils in Cultured Cardiac Myocytes

ANDRZEJ A. DLUGOSZ, PARKER B. ANTIN, VIVIANNE T. NACHMIAS, and HOWARD HOLTZER
Department of Anatomy, School of Medicine, University of Pennsylvania, Philadelphia 19104

ABSTRACT The topographical relationship between stress fiber-like structures (SFLS) and nascent myofibrils was examined in cultured chick cardiac myocytes by immunofluorescence microscopy. Antibodies against muscle-specific light meromyosin (anti-LMM) and desmin were used to distinguish cardiac myocytes from fibroblastic cells. By various combinations of staining with rhodamine-labeled phalloidin, anti-LMM, and antibodies against chick brain myosin and smooth muscle α-actinin, we observed the following relationships between transitory SFLS and nascent and mature myofibrils: (a) more SFLS were present in immature than mature myocytes; (b) in immature myocytes a single fluorescent fiber would stain as a SFLS distally and as a striated myofibril proximally, towards the center of the cell; (c) in regions of a myocyte not yet penetrated by the elongating myofibrils, SFLS were abundant; and (d) in regions of a myocyte with numerous mature myofibrils, SFLS had totally disappeared. Spontaneously contracting striated myofibrils with definitive Z-band regions were present long before anti-desmin localized in the I-Z-band region and long before morphologically recognizable structures periodically link Z-bands to the sarcolemma. These results suggest a transient one-on-one relationship between individual SFLS and newly emerging individual nascent myofibrils. Based on these and other relevant data, a complex, multistage molecular model is presented for myofibrillar assembly and maturation. Lastly, it is of considerable theoretical interest to note that mature cardiac myocytes, like mature skeletal myotubes, lack readily detectable stress fibers.

Stress fibers, consisting of numerous aligned microfilaments with associated contractile proteins, subtend the plasmalemma of many cell types. Electron microscopic studies, combined with heavy-meromyosin decoration, have demonstrated that they consist of long actin filaments periodically interrupted by osmiophilic dense bodies comparable with Z-bands in myofibrils (26, 35, 44, 58). Fluorescent-labeled anti-α-actin or phalloidin stain stress fibers continuously, whereas labeled anti-α-actinin, tropomyosin, and myosin bind in a discontinuous pattern (30, 46, 49, 59, 70). The discontinuous binding of anti-α-actinin and antitropomyosin has been correlated with the periodic distribution of dense bodies seen using electron microscopy. These observations have led to the proposal that stress fibers be viewed as "primitive myofibrils" consisting of tandem, sarcomere-like structures (26, 46, 60). That stress fibers can undergo contraction-relaxation cycles is indicated by changes in their sarcomeric periodicity following exposure to Mg-ATP (46).

Much, however, about the functions of stress fibers remains unknown. Their varying spatial arrangements in cells with different shapes, as well as their persistent absence in rounded, viral transformed cells, suggest a role in cellular cytoarchitecture (6, 52, 61, 67). It has also been proposed that they influence the deployment of other cytoskeletal structures. For example, observations on cultured skeletal myogenic cells recovering from exposure to the carcinogen ethyl methylsulfonate (EMS)[1] revealed striking temporal and topographical relationships between individual SFLS and newly-forming individual striated myofibrils. Briefly, we found that in EMS-recovering myosheets the earliest assembly of thick myosin and thin α-actin filaments occurred in intimate association with a single pre-existing SFLS (2, 41, 42). As additional thick

---

[1] *Abbreviations used in this paper:* CB, cytochalasin-B; CBM, chick brain myosin; EMS, ethyl methylsulfonate; FITC, fluorescein isothiocyanate; LMM, light meromyosin; SFLS, stress fiber-like structures.

and thin filaments were added to the periphery of such nascent myofibrils (20, 31, 33, 34, 54), this association with a single SFLS was lost and concomitantly the formerly prominent SFLS disappeared. With maturation, SFLS were gradually relegated to the growth tips and pseudopodial extensions of the EMS-recovering multinucleated myosheets.

These observations suggested that a single pre-existing SFLS might serve as a transitory assembly site for a single nascent myofibril, which in turn is followed by the gradual disappearance of that SFLS. These results, however, were derived from EMS-treated skeletal muscle cells. We do not know whether these correlations between SFLS and nascent myofibril reflected interactions required for normal myofibrillogenesis or were induced by the carcinogen treatment. Accordingly, in this report we examine the temporal and topographical relationships between nascent and relatively mature myofibrils, and SFLS in normal cultured heart cells. In this unperturbed system, we again find evidence that (a) a single nascent myofibril first assembles along a single SFLS; (b) this intimate association is lost as the individual myofibril matures and is displaced into the sarcoplasm; and (c) in regions of a cardiac myocyte occupied by relatively mature myofibrils there is a total absence of SFLS. These results strongly suggest that SFLS can serve as a locus or scaffold for directing the assembly of nascent striated myofibrils, which then, as the myofibrils mature, disappears. Furthermore, desmin intermediate-sized filaments play no obvious role in assembly of individual striated myofibrils with definitive A-, I-, M-, and Z-bands.

MATERIALS AND METHODS

Cell Culture: Chick cardiac cultures were prepared from 8–10 d embryos using a modification of previously described procedures (8). Hearts were rinsed in a Ca^{2+}- and Mg^{2+}-free balanced salt solution (CMF: 1.5 mM sodium phosphate, 6 mM sodium bicarbonate, 0.137 M NaCl, 2.7 mM KCl, 5.5 mM glucose [pH 7.4]), pericardia were removed, and the ventricular and atrial tissue was minced. Cells were dispersed using repeated enzymatic digestion and harvested. Tissue fragments were incubated in 10 ml of trypsin solution (0.05% trypsin; [Gibco Laboratories, Grand Island, NY] in Ca^{2+}- and Mg^{2+}-free balanced salt solution) for 10 min at 37°C in a humidified incubator. The supernatant from this first incubation, presumably containing dissociated cells damaged during tissue processing, was removed and discarded, with care taken to avoid removing any tissue fragments. Fresh trypsin solution (3.5 ml) was added and the tissue incubated for 8 min. The supernatant, containing dispersed cardiac cells, was removed and placed into a 25-ml volume of chilled (4°C) nutrient medium (5% fetal calf serum, 50 U/ml penicillin, 50 μg/ml streptomycin, and 2 mM glutamine in Eagle's minimal essential medium with Earle's salts; Gibco Laboratories). The remaining tissue fragments were incubated in 3.5 ml of fresh trypsin solution as above and the dispersed cells harvested an additional 3–5 times. Following removal of the supernatant after the final trypsinization, remaining tissue fragments were gently dissociated in 3.5 ml of growth medium by repeated pipetting, combined with the previously harvested cells, and centrifuged for 10 min. The supernatant was discarded, cells were gently resuspended in nutrient medium, and the suspension was filtered through lens tissue to remove any remaining large clumps of cells. The approximate yield was 1–2 million cells per heart.

Cells were grown on glass coverslips at an initial density of 2.0–3.5 × 10^5 cells per 2 ml per 35-mm tissue culture dish; cultures were maintained at 37°C in a humidified 5% CO_2 incubator. The day after plating, nutrient medium was replaced with glutamine-free medium (5% fetal calf serum, 50 U/ml penicillin, and 50 μg/ml streptomycin in Eagle's minimal essential medium). Elimination of glutamine from the medium has been shown to facilitate the culture of cardiac myocytes by greatly reducing the proliferation of cardiac fibroblasts (8). Glutamine-free medium was replaced 1–3 times weekly. Using the above technique, beating cardiac myocytes have been maintained for more than 4 wk in culture. Most observations were made on day 7 cultures. To determine whether a particular condition was more apparent in immature versus mature myocytes, day 7 and day 16 cultures, respectively, were examined.

Antibodies: The properties of the antibodies against muscle-specific light meromyosin (anti-LMM) and desmin (antidesmin) have been described. Briefly, in immunoblots prepared using total extracts of skeletal or cardiac muscle, the affinity-purified anti-LMM binds only to the 200-kd myosin band. In similar immunoblots prepared from smooth muscle or fibroblasts, the anti-LMM does not bind to the 200-kd myosin band. In cytoimmunofluorescence, the anti-LMM binding is largely restricted to the myofibrillar A-bands in postmitotic myoblasts, myotubes, and cardiac myocytes (4, 7, 14, 16, 40). Anti-LMM does not stain the myosin in presumptive myoblasts, smooth muscle, fibroblasts, or other cell types examined. The antidesmin binds to intermediate filaments (IFs) in skeletal, cardiac, and smooth muscle (5), but not to the vimentin intermediate filaments in fibroblasts (3, 4, 19, 39). Antibody against smooth muscle α-actinin was a generous gift from Dr. S. Craig (Johns Hopkins University) and has been described previously (10). In skeletal myogenic cultures, this anti-α-actinin has been shown to bind to the Z-band of postmitotic, mononucleated myoblasts and myotubes (1). Antibody was produced against chick brain myosin (anti-chick brain myosin [CBM]) by using column-purified myosin from chick brain (48) for primary injection of rabbits. Pure myosin heavy chain, obtained by eluting the appropriate band from a 7% SDS gel, was used for boosting the primary injection four times. IgG was purified and found to react with the heavy chains of myosin from fibroblasts and EMS-treated skeletal myosheets, but not with myosin heavy chains from chick myofibrils as demonstrated by immunoblot. Immunofluorescent localization of CBM was limited to stress fibers of chick fibroblasts and EMS myosheets; myofibrils did not bind the anti-CBM (41, 42).

Immunofluorescent Staining: Processing of cells for immunofluorescent staining was carried out as described (4, 64), with minor modifications. Briefly, cultures were rinsed with phosphate-buffered saline (PBS: 5 mM sodium phosphate, 0.15 M NaCl [pH 7.3]) and fixed for 3 min in 2.5% formaldehyde in PBS. The cells were then rendered permeable and soluble proteins extracted using PBS containing 0.5% Triton X-100 (Sigma Chemical Co., St. Louis, MO). This solution was used for this step and all subsequent antibody "washes," and was replaced three times for a total of at least 30 min during each step. Various sequences of antibody or reagent incubations were used to produce the several double-stained preparations analyzed in this study. For antidesmin, anti-CBM, and anti-α-actinin, the indirect immunofluorescent technique was used, while the fluorescein isothiocyanate (FITC)-labeled anti-LMM was visualized directly. To stain the same cells with anti-LMM and another antibody, a previously described procedure was used (4, 64). The appropriate dilution of the antibody to be visualized indirectly was applied first. This, and all other antibody incubations, were carried out for 30–40 min at 37°C in a humid chamber. After the primary antibody incubation, cells were washed three times, incubated with secondary antibody (rhodamine-labeled goat anti-rabbit IgG [Cappel Laboratories, Inc., Cochranville, PA]), and washed again. Prior to application of anti-LMM, the cells were incubated for 15–20 min at room temperature in a 1:5 dilution of normal rabbit serum in PBS to saturate exposed goat anti-rabbit IgG sites. Cells were then incubated with anti-LMM, washed, and mounted using 1:1 glycerol/PBS. Rhodamine-phalloidin (Molecular Probes, Inc., Junction City, OR), which binds specifically to F-actin (52, 70), was used to visualize microfilaments in the form of stress fibers and thin filaments within myofibrils. In antibody-stained preparations counterstained with rhodamine-phalloidin, fluorescein was used for the antibody visualization. Following the final wash, cultures were rinsed repeatedly with PBS, incubated for 20 min at room temperature in 10 U/ml phalloidin in PBS (2 U/coverslip), washed several times in PBS, and mounted as above. In some preparations, the fluorochrome bisbenzimide Hoechst 33258 was used to stain nuclei (64). Cells were examined with a Zeiss epifluorescence microscope using appropriate filters for either fluorescein or rhodamine fluorescence.

RESULTS

Chick Cardiac Cultures

Several hours after plating, the cells exhibited two distinct morphologies. Cardiac myocytes, occasionally observed beating, were spherical, while fibroblastic cells were flattened and somewhat polygonal in shape. By the second day in culture, most myocytes also flattened but were readily distinguished from fibroblastic cells by virtue of their greater phase-density and large glycogen vacuoles. After several days in culture, striated myofibrils and occasionally SFLS were visible in the living, irregularly-shaped myocytes; nonmuscle cells also occasionally exhibited prominent SFLS. Early during the culture

period, myocytes were typically observed as single mononucleated cells; but with time, oligonucleated cells as well as aggregates consisting of several to more than 40 cells, were increasingly apparent. Both single cells and cell aggregates exhibited spontaneous beating in culture, with a typical frequency of 80 beats per minute when examined at room temperature. Ultrastructural studies of these cardiac myocytes revealed many branching, individually striated myofibrils consisting of interdigitating thick and thin filaments as well as conspicuous intercalated disks. The length of thick and thin filaments and the Z-bands of these sarcomeres were, in readily discernable details, indistinguishable from those in mature cardiac myocytes.

FITC-labeled anti-LMM was used to differentiate between cardiac myocytes and the other cells in the population. Myocytes were defined as cells binding both antidesmin and anti-LMM in either a nonstriated or striated distribution. Cells binding antidesmin, but not concurrently binding anti-LMM,

are considered to be smooth muscle cells (5). Cells that did not bind anti-LMM or antidesmin will be referred to as fibroblastic. The number of myocytes increased several-fold over the first 5 d in culture, reflecting the continued proliferation of differentiated myocytes growing in vitro (9, 51). The population of cells being studied thus enabled us to evaluate various stages of cardiac myogenesis within a given culture and even within a single cell. Thus, "mature" myocytes, containing a relatively large number of sizable, anti-LMM positive myofibrils, were present in day 7 as well as day 16 cultures, along with "immature" myocytes exhibiting fewer, thinner myofibrils.

Localization of Anti-LMM and Antidesmin

Anti-LMM bound almost exclusively to myofibrillar A-bands (Fig. 1, a and c). The sarcomeric periodicity of 2.0–2.5 μm, characteristic of all striated myofibrils, was observed in
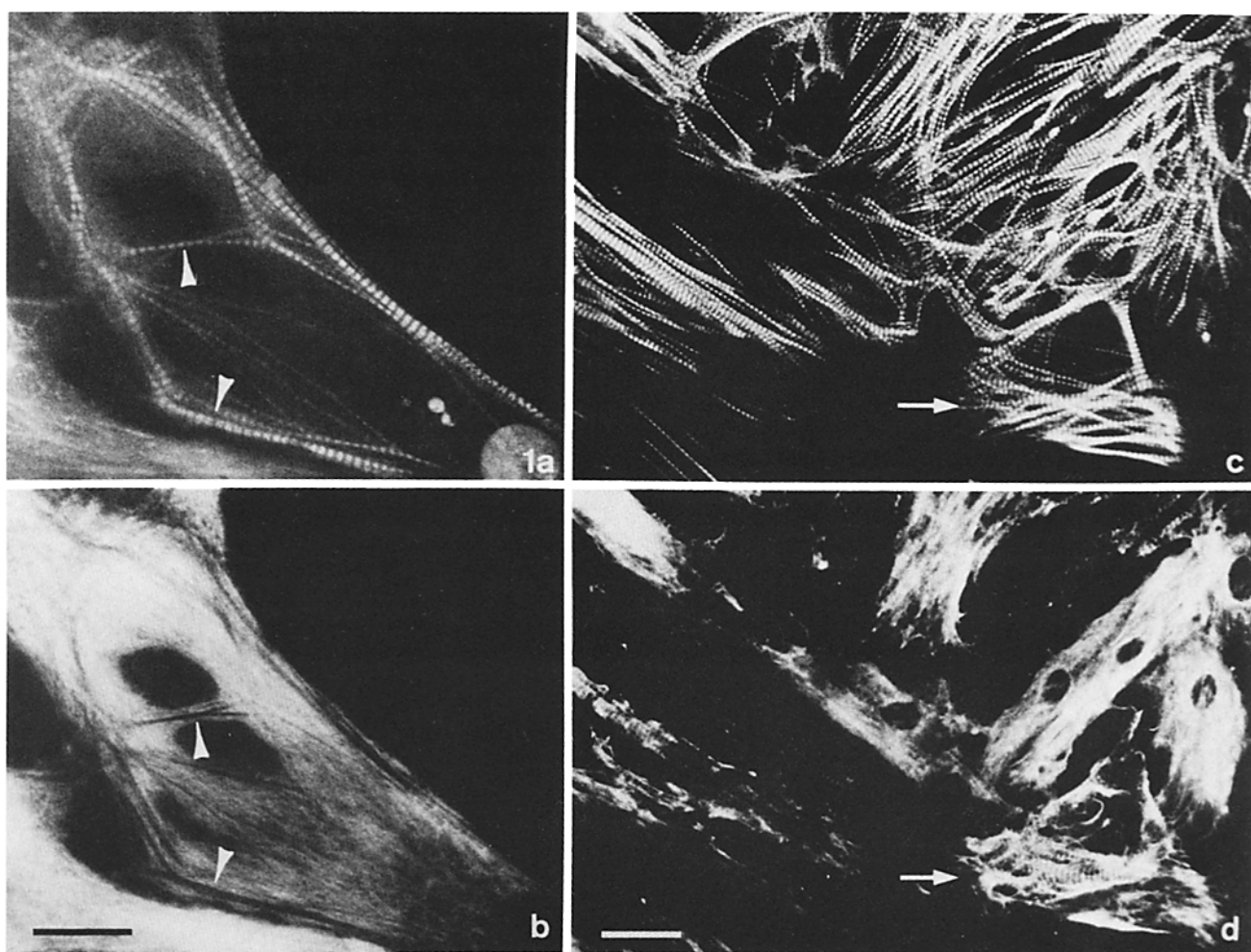

FIGURE 1   (a and b) The same relatively immature cardiac myocyte visualized with both directly labeled FITC-anti-LMM (a) and indirectly labeled rhodamine-antidesmin (b). The anti-LMM binding is restricted to myofibrillar A-bands as illustrated in a, whereas antidesmin stains a dense filamentous network present throughout most of the sarcoplasm (b). Note the striking exclusion of antidesmin binding in most regions of this cell which are occupied by definitively striated myofibrils (arrowheads). At this stage of myofibrillogenesis there is no obvious localization of desmin to the I-Z region of these emerging myofibrils. × 690. Bar, 20 μm. (c and d) Fluorescence images of the same microscopic field illustrating several relatively mature cardiac myocytes visualized with both anti-LMM (c) and antidesmin (d). Note the abundance of anti-LMM-positive myofibrils in these myocytes. In many cells, the antidesmin binds to an extensive filamentous network throughout the cytoplasm and exhibits no obvious relationship to the definitively striated myofibrils. Other cells in the same field bind antidesmin to the I-Z region of some of their larger myofibrils as well as throughout their sarcoplasm (arrows) Bar, 25 μm. × 440.

nascent myofibrils of considerably < 0.5 μm-diam (1, 31), as well as in more mature myofibrils many microns in diameter (33, 35). Individual myofibrils of various diameters co-existed in a single myocyte. Complex branching and criss-crossing of individual myofibrils was conspicuous. Numerous myocytes exhibited areas of cytoplasm rich in myofibrils, whereas in other regions of the same cell myofibrils were totally absent. Thus, in the same myocyte it was possible to compare (a) fine, newly assembled myofibrils with those of greater diameter, and (b) regions rich in myofibrils with those totally lacking myofibrils.

There was a redistribution of desmin over time in cardiac myocytes. Fig. 1a illustrates a relatively immature cardiac myocyte with several anti-LMM-positive myofibrils coursing through its cytoplasm. The antidesmin stained a dense overlapping network of fine filaments which filled much of this cell's cytoplasm, but was entirely excluded from those regions occupied by myofibrils (Fig. 1, a and b). It did not bind to or stain any of the numerous definitive Z-bands present in these myofibrils. No periodic linkage with the sarcolemma via desmin-positive filaments was evident in these immature myocytes. Ultrastructural studies confirmed these cytoimmunofluorescent findings. 100 pairs of Z-bands, each pair consisting of adjacent Z-bands on neighboring myofibrils, were examined for transverse, linking, 10-nm filaments. None were found. In striking contrast, longitudinally oriented, 10-nm filaments were numerous (eg. reference 44). Similarly, if 10-nm filaments periodically linked individual Z-bands to the sarcolemma, they were not readily detected in our electron microscope sections.

On the other hand, in relatively mature myocytes the antidesmin, in addition to binding to longitudinally-oriented filaments, also stained the I-Z region (arrowheads in Fig. 1, c and d). Although the sarcomeric antidesmin staining pattern was more common in day 16 than day 7 cultures, and more frequently observed along the larger myofibrils of a given cell, we were not able to detect any other consistent relationship between anti-LMM-positive myofibrils and localization of antidesmin to the I-Z region. It is noteworthy that in double-stained preparations no relationship was observed between SFLS and structures binding antidesmin. A similar shift of desmin from longitudinal fibers of indefinitive length to the I-Z band was previously reported for both skeletal (4, 19, 23, 39, 50, 65) and cardiac (22) myogenic cells.

Binding of Phalloidin in Chick Cardiac Cultures

Although the fibroblastic cells and myocytes both bound phalloidin, the patterns obtained in the two cell types were distinctly different. Phalloidin stained the prominent stress fibers in fibroblastic cells in a continuous, nonperiodic fashion (Fig. 2). These stress fibers often occurred in two or more well-separated planar groups, the fibers within a group often arranged in parallel, and at other times in a fan-like distribution (Fig. 2a). Frequently, the most prominent group of stress fibers was arranged along the ventral surface of the cell. In many fibroblastic cells (~10-20%), polygonal networks were conspicuously located just beneath the upper surface of the cell (Fig. 2b). Both vertices and the interconnecting fibers of these networks bound phalloidin, consistent with previous immunofluorescent and ultrastructural studies demonstrating actin in both locations (27, 49, 59). Frequently, irregular patches 2-5-μm diam located along a cell's outermost edge were intensely phalloidin-positive, reflecting the abundance of microfilaments in ruffled membranes (30, 62). It is to be emphasized that in these fibroblastic cells, virtually the entire plasmalemma was underlined by phalloidin-positive stress fibers. In no instances were large expanses of the cells' surfaces without numerous underlying stress fibers.

We have reported that phalloidin stains both the putative β- and α-actin filaments in transitory SFLS of skeletal myogenic cells and the polymerized α-actin comprising the thin filaments of skeletal myofibrils (41, 42). The pattern of binding in these two structures is so different, however, that in the same cell, SFLS are readily distinguished from striated myofibrils. Similarly, in a single cardiac myocyte, as demonstrated in Fig. 3, the continuous staining of SFLS was readily distinguished from the sarcomeric staining pattern of myofibrils. In relaxed myofibrils the distance between unstained H-bands was ~2.5 μm. In contracted myofibrils the contraction bands yielded an even more intense but complex, periodic staining pattern that was also unique to striated myofibrils (data to be published elsewhere).

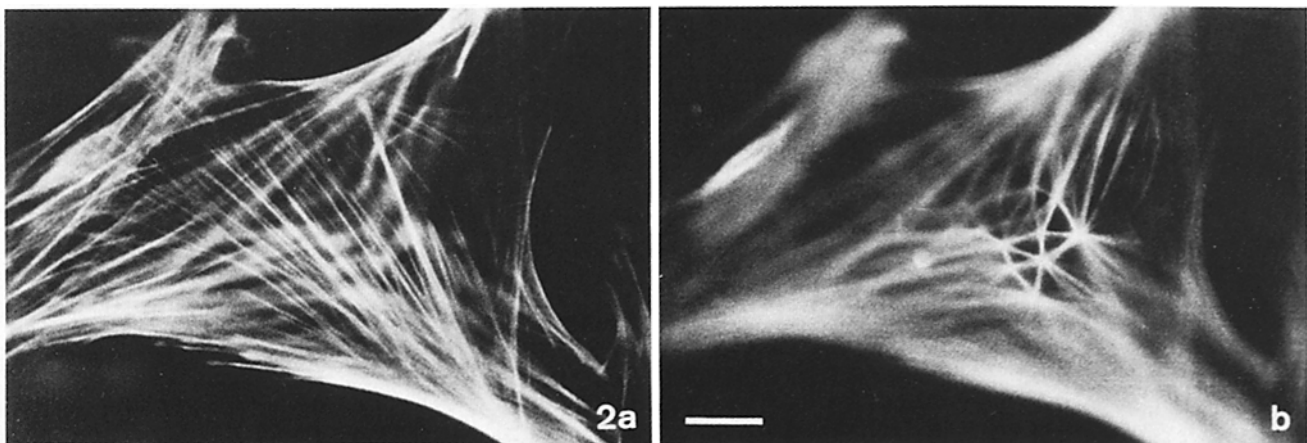In contrast to their widespread distribution in fibroblastic

FIGURE 2   Two optical sections through the same fibroblastic cell illustrating two common arrangements of the phalloidin-positive stress fibers. Long, continuously stained stress fibers are present on the inner aspect of this cell's membrane in close proximity to the substrate (Fig. 2a). A continuously stained polygonal network located in the uppermost portion of this cell is illustrated in Fig. 2b. × 1,010. Bar, 10 μm. × 1,010. These findings confirm earlier reports to the effect that definitive Z-bands assemble and function well before desmin IF localize to the I-Z region (4, 19, 39, 65).
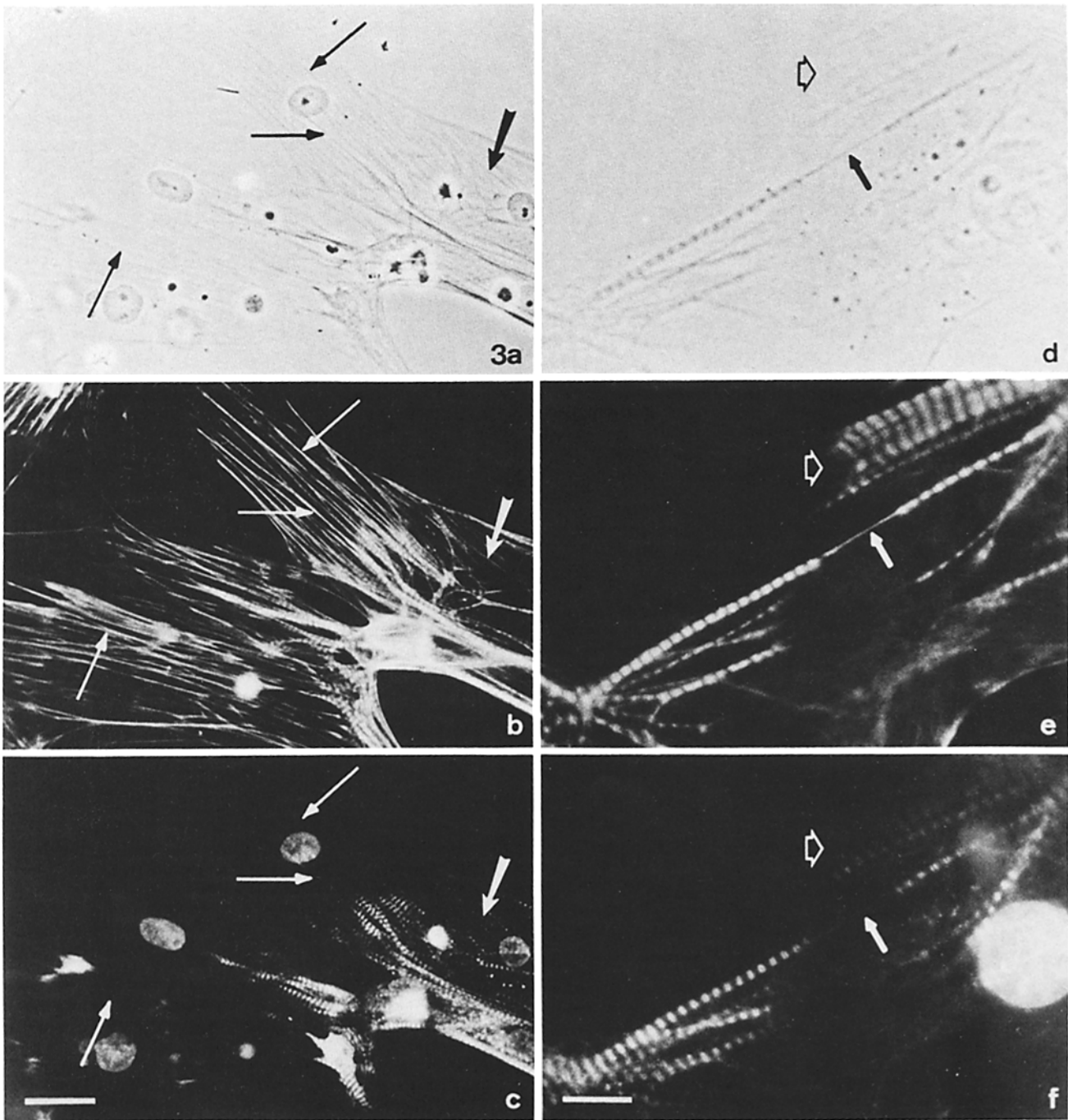
FIGURE 3   (a-c) A phase and corresponding fluorescence micrographs of two adjacent immature cardiac myocytes stained with rhodamine-phalloidin (b) and FITC-labeled anti-LMM (c). Thin arrows indicate a large number of fine, individual phalloidin-positive SFLS, many of which are continuous with single phalloidin-positive striated myofibrils. The interrupted sarcomeric pattern of the myofibril stained with phalloidin, and the uninterrupted pattern of the SFLS stained with phalloidin, permit unambiguous identification of the two structures (b). The excellent coincidence of individual striated myofibrils as visualized with either phalloidin (b) or anti-LMM (c) is evident. Note the 2-10-μm stretch where a single SFLS overlaps its associated single myofibril. Observe also that regions with many criss-crossing myofibrils have lost most of their SFLS (large arrows). Nuclei are visualized using bisbenzimide. (d-f) A phase and corresponding fluorescence micrographs of a single, relatively mature cardiac myocyte stained with rhodamine-phalloidin (e), FITC-labeled anti-LMM, and bisbenzimide (f). Larger arrow indicates a broad, flat, well-striated myofibril that terminates at the cell's membrane; the latter is not visible in this micrograph. Two definitively striated myofibrils, as visualized with phalloidin, are connected by a persisting phalloidin-positive SFLS (e; small arrows). This phalloidin-positive SFLS does not bind the anti-LMM (f). Note also the general absence of phalloidin-positive SFLS in this relatively mature myocyte. Bars, 25 μm (a-c); 10 μm (d-f). × 440 (a-c); × 1,100 (d-f).

cells, the over-all distribution of SFLS varied greatly from myocyte to myocyte. Immature myocytes, characterized by only a few thin nascent myofibrils, were rich in phalloidin-positive SFLS. In contrast, more mature myocytes with many striated, broader myofibrils could be totally devoid of SFLS. Even within a single cell, a region containing mature myofibrils would have totally lost its SFLS, whereas a region not yet penetrated by elongating myofibrils would still display

prominent SFLS. In most mature myocytes phalloidin was strictly limited to staining the edge of a ruffled membrane and/or the cell's growth tip. Fig. 3, a–c illustrates several findings relevant to the spatial distribution of SFLS and myofibrils in two relatively immature myocytes: (a) single, long, phalloidin-positive SFLS, visualized by their continuous staining distally, merge into phalloidin-positive single myofibrils, visualized by their distinct, sarcomeric staining proximally (Fig. 3, a and b); (b) in regions of the myocyte not yet occupied by the elongating myofibrils, phalloidin-positive SFLS were abundant and similar to those found in fibroblastic cells (thin arrows in Figs. 3a and 6); (c) in contrast, in regions within a given myocyte where phalloidin-positive mature myofibrils dominated, phalloidin-positive SFLS were absent (see below); and (d) often, in double-stained preparations, a single, fine, striated myofibril, as visualized with anti-LMM, overlapped for distances of 2–10 μm a single SFLS stained with phalloidin (compare Fig. 3, b and c). Fig. 3, d–f illustrates a more mature myocyte with two well-separated striated myofibrils linked by a single, persisting phalloidin-positive SFLS. Note that the remainder of this mature myocyte has lost virtually all of its SFLS. Proximal SFLS in continuity with distal striated myofibrils (Figs. 3d, 3) are rare compared with the usual, continuous distal SFLS continuous with proximal striated myofibrils. But it does suggest a bi-directionality with respect to elongation of myofibrils, as probably occurs during regeneration. Phalloidin-positive SFLS were generally, though not always, also anti-CBM- and anti-α-actinin-positive (see below). It should be emphasized that the polygonal networks seen in fibroblastic cells (Fig. 2b) have not been observed in myocytes.

Localization of Anti-CBM

Anti-CBM bound to all cells in these cultures albeit faintly in some myocytes. In fibroblastic cells, three distinct fluorescent patterns were observed: (a) stress fibers; (b) submembranous sheet-like arrays with a periodicity of ~0.6 μm; and (c) a finely granular cytoplasmic haze. As observed with phalloidin, anti-CBM bound to stress fibers that were arranged in planar groups (Fig. 4b). However, unlike the continuous staining with phalloidin, anti-CBM bound to stress fibers in a finely punctate manner discernable only using high magnification. A number of fibroblastic cells bound the anti-CBM to submembranous polygonal networks like those seen with rhodamine-phalloidin (Fig. 4d). We also found, as reported by others (27, 59), that the vertices of these networks did not bind the anti-CBM. In a single fibroblastic cell, stress fibers commonly merged into striated sheet-like arrays (see also 18, 30, 71).

Myocytes also bound anti-CBM to SFLS, striated sheet-like arrays, and fine cytoplasmic granules. However, the density, distribution, and staining characteristics of the anti-CBM-positive SFLS in myocytes differed from those in the fibroblastic cells in several respects: (a) they rarely formed the numerous clusters of long, unbranched parallel fibers so commonly found in fibroblastic cells; (b) in some myocytes they could be relegated to relatively limited regions of the cell, whereas in others they had completely disappeared (Figs. 4, b and e); (c) they occasionally pursued a curvilinear, branching course similar to that displayed by cardiac myofibrils; and (d) in many myocytes examined, the periodicity of anti-CBM-positive SFLS was more distinct than in fibroblastic cells.

Anti-CBM-positive SFLS, like phalloidin-positive stress fibers, were most prominent in immature myocytes and in regions of mature myocytes that lacked myofibrils (Fig. 4, b, c, e, and f). Often the striated myofibrils tended to be confined to one large area of the cell: in these cells virtually all of the SFLS were confined to the area lacking myofibrils. In fact, the complementary staining with the two myosin antibodies was often quite remarkable. A comparable inverse and complementary distribution of nonmuscle myosin and skeletal myosin has previously been demonstrated in normal developing rat myotubes (18). As with phalloidin, areas of overlapping staining were present in regions of the cell where an anti-LMM-positive myofibril ended and an anti-CBM-positive SFLS persisted (Fig. 4, b and c). In contrast to its distribution in SFLS, the diffuse, cytoplasmic staining with anti-CBM was observed throughout the cell irrespective of the presence or absence of myofibrils. As observed in fibroblastic cells, CBM-positive submembranous sheets exhibiting a crisp, fine periodicity (~0.6 μm) were occasionally seen in myocytes (Fig. 4b, inset). These structures were continuous with individual SFLS, and were notably more prominent in regions of the cell lacking myofibrils. The fine periodicity of these structures cannot be confused with that of nascent myofibrils (~2.5 μm). Again it is worth noting that polygonal networks were not observed in myocytes stained with anti-CBM.

Localization of Anti-α-actinin

Like the anti-CBM, anti-α-actinin bound to all fibroblastic cells as well as myocytes, but again the binding pattern differed in the two groups of cells (Fig. 5). Anti-α-actinin bound to SFLS in a punctate fashion visible under high power. As demonstrated with phalloidin and anti-CBM, SFLS binding anti-α-actinin were plentiful in fibroblastic cells. A diffuse, granular cytoplasmic fluorescence was also present in nonmuscle cells, extending to the cells' borders. Polygonal networks were visualized in fibroblastic cells using this antibody. Consistent with previous studies (27, 49, 59), binding was most prominent in the vertices of the network, though the connecting fibers were also occasionally anti-α-actinin positive.

All myocytes with well-formed myofibrils, as visualized with anti-LMM, invariably bound anti-α-actinin to thin, distinct bands corresponding to the Z-line of definitively-striated muscle sarcomeres (Fig. 5, a and b). Such anti-α-actinin stained Z-bands exhibited a 2–2.5-μm periodicity. In myocytes the distal end of a long anti-α-actinin-positive fiber might exhibit the fine punctate pattern of a SFLS, but exhibit a Z-band periodicity at the other end. In such instances, the latter end would also be LMM-positive. Once again, myocytes with well-formed myofibrils exhibited relatively few anti-α-actinin-positive SFLS when compared with fibroblastic cells (Fig. 5, a and b). It is worth emphasizing that as with the other fluorescent reagents, the anti-α-actinin did not reveal the presence of polygonal networks in LMM-positive myocytes.

DISCUSSION

Earlier studies on myofibrillogenesis in postmitotic, mononucleated skeletal myoblasts and immature myotubes focused on events occurring in their growth tips. It was concluded that within this circumscribed domain, (a) newly polymerized
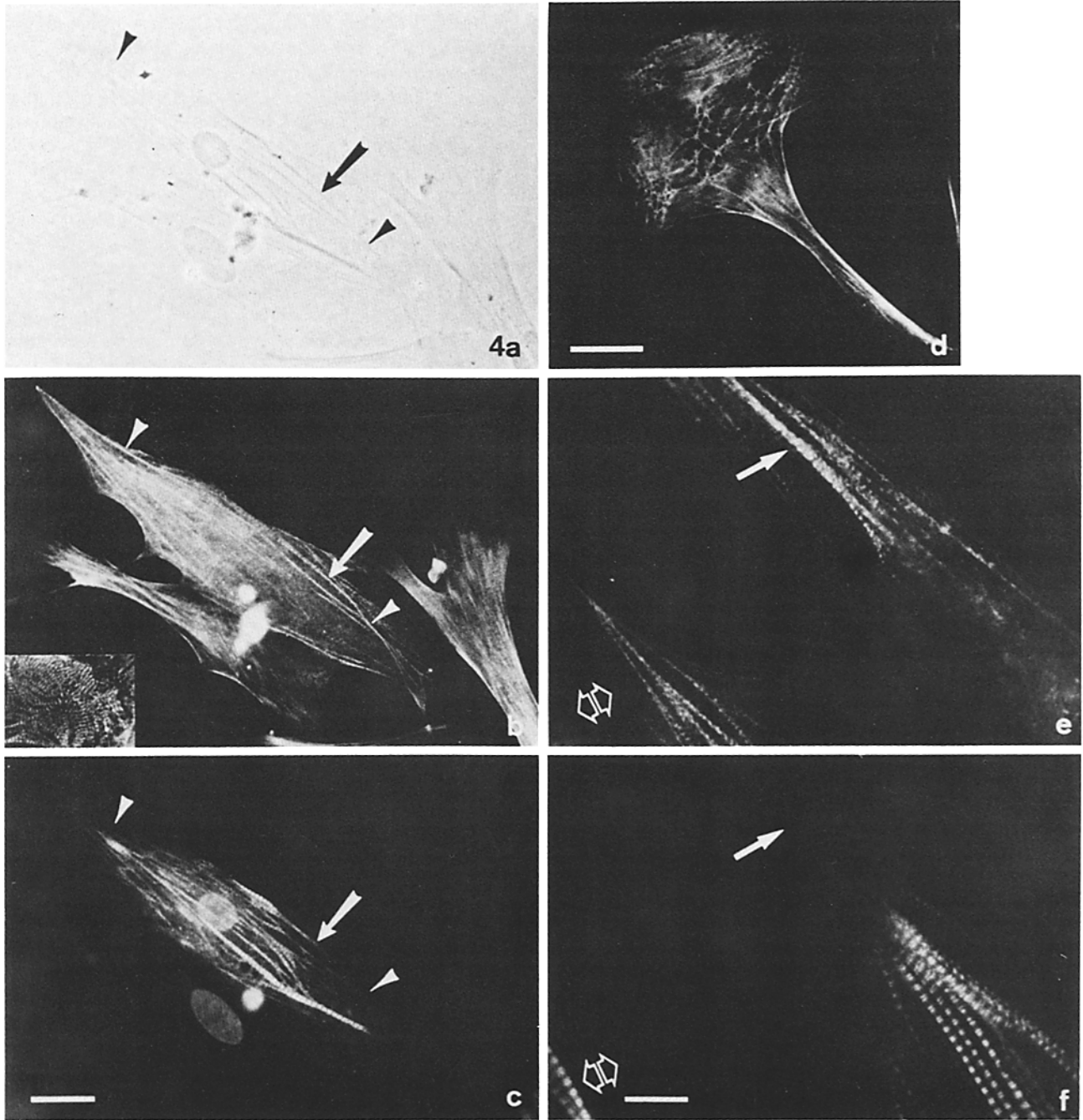
FIGURE 4 (a–c) A phase and corresponding fluorescence micrographs of three fibroblastic cells and one myocyte stained with indirectly labeled rhodamine-anti-CBM (b), FITC-labeled anti-LMM, and bisbenzimide (c). All four cells bind the anti-CBM (b), but only the myocyte binds the anti-LMM to nascent and relatively mature striated myofibrils (c). Arrowheads point to the punctate staining of several prominent CBM-positive SFLS in the myocyte. Inset in b illustrates a particularly complex arrangement of an anti-CBM-positive submembranous sheet. The considerable overlap between some of the disappearing SFLS and the nascent myofibrils can be appreciated by comparing b with c (arrows). (d) A single fibroblastic cell stained with anti-CBM. Virtually the entire cell binds the antibody to submembranous stress fibers, striated sheets, and polygonal networks. At higher magnifications, the vertices of the polygonal networks proved to be negative with the anti-CBM. (e and f) Fluorescence micrographs illustrating part of a cardiac myocyte stained with rhodamine-anti-CBM (e) and FITC-anti-LMM (f). These micrographs illustrate the striking complementarity in the distribution of SFLS and striated myofibrils characteristic of relatively mature myocytes. Thin arrow indicates the punctate appearance of the anti-CBM-positive SFLS (e). The SFLS gradually disappear in the region occupied by striated myofibrils (f). The broad arrows indicate one region where a cluster of SFLS courses parallel to a cluster of nascent myofibrils. Bar, 25 μm (a–d); 10 μm (e and f); × 400 (a–c); × 460 (d); × 1,010 (e and f); × 610 (inset).

thick and thin filaments were rapidly organized into interdigitating arrays and (b) "new" definitive-sized sarcomeres were added in an incremental fashion to the ends of fine, elongating, individual, nascent myofibrils (31–33, 54). As determined by antibody staining, the apparently unstriated end of a single nascent myofibril abruptly terminated in the cell's growth tip. Subsequent studies have emphasized the morphological complexity of these growth tips. In addition to the ends of nascent
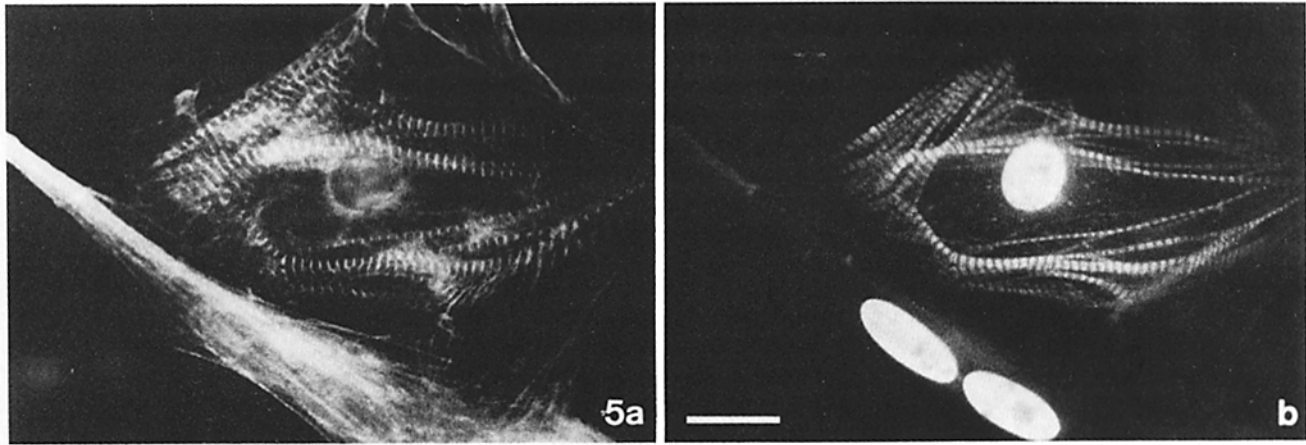
FIGURE 5 Fluorescence micrographs of the same microscopic field illustrating a cardiac myocyte and fibroblastic cell stained with indirectly labeled rhodamine-anti-α-actinin (a), FITC-anti-LMM, and the nuclear stain bisbenzimide (b). Anti-α-actinin-positive SFLS are abundant in the binucleated fibroblastic cell (a). In contrast, anti-α-actinin is most prominently bound to the Z-band of striated myofibrils in the myocyte, which exhibits relatively few SFLS (a and b). Bar, 20 μm. × 640.

myofibrils, they harbor a bewildering tangle of microfilaments, organized SFLS, desmin and vimentin intermediate filaments, and microtubules (1, 14, 18, 40, 56). In terms of binding anti-LMM, phalloidin, anti-CBM, anti-α-actinin, and antidesmin, growth tips of cardiac myocytes, though smaller and multiple, are basically similar to growth tips in skeletal myogenic cells (e.g., Fig. 3, a-c). These morphological findings raise the question whether these different sets of filaments play a role organizing myofibrils.

That SFLS participate in the assembly of nascent myofibrils was demonstrated by observing myogenic cells recovering from an EMS-blockade (2, 41, 42). Skeletal myogenic cells in EMS form immense, multinucleated myosheets ribbed with numerous, long, very prominent SFLS. As the carcinogen selectively blocks the synthesis of myofibrillar isoforms, these myosheets lack myofibrils. After the drug is removed the synthesis of myofibrillar isoforms is initiated. Early in recovery, there is a one-to-one topographical association between a single, nascent myofibril and a single, pre-existing, prominent SFLS. As the individual myofibril increases in girth this association is lost, and the previously conspicuous SFLS totally disappears.

The observations in this study on cultured cardiac myocytes on the waxing and waning of SFLS and the emergence of myofibrils extend those reported for recovering EMS-myosheets and normal myotubes (2, 18, 41, 42). In cultured myocytes individual proximal nascent myofibrils demonstrated continuity with, and overlapped for many microns, distal individual SFLS. Such SFLS did not bind the anti-LMM, but bound phalloidin in a continuous fashion, and the anti-CBM and anti-α-actinin in a discontinuous fashion. Relatively immature myocytes lacking sizable myofibrils generally displayed many prominent SFLS. Conversely, mature myocytes that had assembled many sizable myofibrils lost all their SFLS. This striking reciprocal relationship between the presence of striated myofibrils and the complete absence of overlying SFLS was evident even in different regions within a single myocyte.

Fig. 6 presents our findings in the form of a model which summarizes hypothesized sequential interactions between SFLS, myofibrils, and the sarcolemma during early stages of myofibrillogenesis. The period denoted by t_1 was experimen-

tally induced, and documented by electron microscope cross-sections only in EMS-treated skeletal cells (41, 42). A comparable period has not been systematically studied in cardiac myocytes for prior to being cultured the majority of myocytes had already assembled some fraction of their myofibrils (17, 51, 63).

Fig. 6 postulates at least two phases in the assembly of definitively striated myofibrils. Phase I, or the period t_2, involves the earliest assembly of small numbers of thick and thin filaments in proximity to a single SFLS. These thick filaments are 1.5 μm long, and even when numbering less than two dozen, are already stacked into irregular A- and I-bands (Tokunaka and H. Holtzer, in preparation). During phase II, or periods t_3-t_4, the nascent myofibril is displaced from its subcortical domain while the SFLS to which it had been linked gradually disappears. Subsequently vast numbers of newly-assembled thick and thin filaments are added to the periphery of the nascent myofibril, maintaining the earlier determined sarcomeric pattern (21, 31-34). Relative to the millions of thick and thin filaments that will be assembled as the myofibril increases in length and girth, obviously only a vanishingly small number would be assembled in phase I. Judging from observations on postmitotic, mononucleated skeletal myoblasts, phase I for a given myofibril can be completed in <10 h (1, 34, 36, 40, 54). Observations of living postmitotic myoblasts under the polarizing microscope revealed that 10-30 new, definitively-sized sarcomeres can be added to the tips of a single myofibril in 24 h (unpublished data).

The ability of myosin and actin monomers to self-assemble into thick and thin filaments is well documented (25, 29, 43, 45). Presumably the scaffold-like function postulated for SFLS or for nascent myofibrils would depend in part on the self-assembling properties of the myofibrillar isoforms. SFLS and nascent myofibrils would primarily determine where in the cell myofibrillar isoforms actually polymerize, interact to form cross bridges, allow Z-band proteins to assemble, etc. An obvious question is whether, in the absence of SFLS or nascent myofibrils, the myofibrillar isoforms would self-assemble into tandem sarcomeres? The effects of cytochalasin-B (CB) on developing muscle cells are germane to this question. CB fragments stress fibers into intense phalloidin-posi-

Dense Bodies
Nascent myofibril
(α-actin, thick
myosin filament,etc.)

Z-Bands

Vimentin and desmin 10 nm filaments

Mature myofibril

├─ t₁ ─┼─────── t₂ ────────┼──────────── t₃ ─────────────┼──── t₄ ───

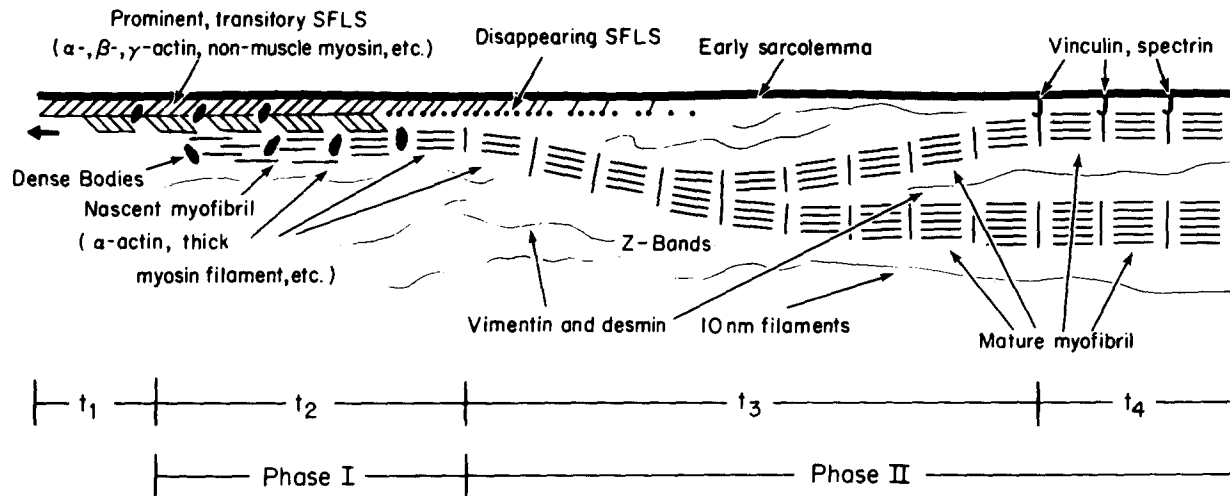├─────── Phase I ────────┼────────────── Phase II ──────────────

FIGURE 6 A simplified scheme depicting several relatively early sequential events leading to two definitively striated myofibrils; one associated with, the other not associated with, the sarcolemma. The large arrow pointing to the left indicates the usual direction of myofibril elongation in an elongating cell. The nascent myofibril forms in intimate association with a single, pre-existing SFLS during Phase I. As the myofibril increases in girth by the peripheral addition of thick myosin and thin actin filaments and other myofibrillar proteins, its association with the SFLS is lost (early Phase II). It is worth emphasizing that the absolute dimensions of the A-, I-, Z-, M-, and H-bands that characterize the nascent myofibrils are virtually indistinguishable from those observed in mature muscle. Tandem arrays of these definitive sarcomeres are present at a time when desmin and vimentin are present as longitudinal filaments of indeterminate length distributed throughout the sarcoplasm. Desmin does not link the Z-bands of these early myofibrils together nor does it anchor them to the sarcolemma. The gradual disappearance of SFLS might not be directly linked to myofibrillogenesis. Instead it might indirectly be due to the multiple structures occupying and requiring a relatively rigid sarcolemma and sub-cortical domain (periodic invaginations of the T-system, anchored Na⁺ and Ca⁺² channels, etc.). Presumably, the presence of such morphological entities would preclude the assembly or persistence of structure even as labile as SFLS. Note the irregular geometry of the dense body-like structures that associate with both SFLS and 1.5-μm long thick filaments. The first polymerized thick filaments are not laterally aligned. The SR, not shown, is prominent at the I-Z region of even nascent, striated myofibrils. For additional details see text.

tive patches (52, 69). Postmitotic mononucleated and binucleated myoblasts reared in CB developed into round, spontaneously pulsating cells, as did cardiac cells in CB (12, 34, 36), (unpublished data). Though small organized arrays emerged, for the most part the bridged thick and thin filaments in CB-treated cells appeared almost randomly scattered. Studies in which the resting potential was experimentally perturbed also demonstrated the need for normal membrane activity in the assembly of nascent myofibrils (11).

Fig. 6 suggests interactions between actin and myosin isoforms of SFLS and of myofibrils. For example, α-actin might be incorporated onto the ends of short filaments of the β- and γ-actins that together comprise the pre-existing SFLS; alternatively, the β- and γ-actins of the stress fiber might serve as a template for the polymerization of α-actin into a homopolymeric myofibrillar thin filament. A fractionally higher binding constant of α-actin over β- or γ-actin for myofibrillar thick filaments would gradually segregate early thick and thin filaments from their associated SFLS. The inverse and complementary relationship between SFLS and myofibrils might also reflect the increased synthesis of the myofibrillar isoforms as the synthesis of the nonmyofibrillar isoforms declines in maturing myogenic cells. Recent findings are pertinent to these possibilities: (a) 10 min after microinjection, actin prepared from skeletal muscle (presumably α-actin) localized to the stress fibers of fibroblasts (24) and chicken gizzard cells (47); (b) the product of a cloned cardiac actin gene introduced into fibroblasts was incorporated into the Triton X-100 insoluble fraction to the same extent as endogenous β- and γ-

actins (28). Gordon et al. (25) have demonstrated in vitro co-polymerization of actins obtained from Acanthamoeba and skeletal muscle. Whether there is a period during which α-actin can co-polymerize in situ with the β- and γ-actins in SFLS remains to be determined.

Fig. 6 suggests that linking individual, definitively striated myofibrils to one another and to the sarcolemma occurs secondarily, long after the formation of A-, I-, and Z-bands. This view is supported by the dramatic redistribution of desmin as muscle matures (4, 22, 23, 39, 65). In early postmitotic myoblasts desmin is distributed throughout the cell. With maturation, the filaments align parallel to, and between, the striated, spontaneously contracting myofibrils. Days later, and long after the formation of Z-bands, desmin secondarily localizes to the I-Z-bands of definitive myofibrils. These observations argue against an essential role for desmin in assembling Z-bands. On the other hand, it will be interesting to learn about how and when myofibrils are linked to the sarcolemma by way of vinculin (55), and spectrin (53).

Currently it is difficult to differentiate rigorously between stress fibers and microfilaments, although the former are generally viewed as more static. Stress fibers and/or microfilaments, as well as having a skeletal role, are believed to be involved in substrate adhesion, receptor mobility, and pinocytosis (58, 66, 68). Mature cardiac and skeletal muscle cells must appropriately deploy their membrane receptors and they avidly pinocytose sucrose and phagocytose latex particles (15, 37, unpublished observations). Can microfilaments, too fine to be detected by phalloidin, be mobilized to function as do

stress fibers in fibroblastic cells? Clearly, much is yet to be learned of what stress fibers and/or microfilaments do and how they do it.

REFERENCES

1. Antin, P. B., S. Forry-Schaudies, T. M. Friedman, S. J. Tapscott, and H. Holtzer. 1981. Taxol induces postmitotic myoblasts to assemble interdigitating microtubule-myosin arrays that exclude actin filaments. *J. Cell Biol.* 89:300-308.
2. Antin, P., and H. Holtzer. 1982. Reversible blocking of myogenesis by a chemical carcinogen. *Anat. Rec.* 202:8 a. (Abstr.)
3. Bennett, G. S., S. A. Fellini, and H. Holtzer. 1978. Immunofluorescent visualization of 100 Å filaments in different cultured chick embryo cell types. *Differentiation.* 12:71-82.
4. Bennett, G. S., S. A. Fellini, Y. Toyama, and H. Holtzer. 1979. Redistribution of intermediate filament subunits during skeletal myogenesis and maturation in vitro. *J. Cell Biol.* 82:577-584.
5. Berner, P., E. Frank, H. Holtzer, and A. P. Somlyo. 1981. The intermediate filament proteins of rabbit vascular smooth muscle: immunofluorescent studies of desmin and vimentin. *J. Muscle Res. Cell Motil.* 2:439-452.
6. Buckley, I. K. 1981. Fine-structural and related aspects of nonmuscle-cell motility. *Cell Muscle Motility* 1:135-203.
7. Chi, J. C., S. A. Fellini, and H. Holtzer. 1975. Differences among myosins synthesized in non-myogenic cells, presumptive myoblasts, and myoblasts. *Proc. Natl. Acad. Sci. USA.* 72:4999-5003.
8. Clark, W. A., Jr. 1976. Selective control of fibroblast proliferation and its effects on cardiac muscle differentiation in vitro. *Dev. Biol.* 52:263-282.
9. Claycomb, W. C., and H. D. Bradshaw, Jr. 1983. Acquisition of multiple nuclei and the activity of DNA polymerase a and reinitiation of DNA replication in terminally differentiated adult cardiac muscle cells in culture. *Dev. Biol.* 99:331-337.
10. Craig, S. W., and J. V. Pardo. 1979. Alpha-actinin localization in the junctional complex of intestinal epithelial cells. *J. Cell Biol.* 80:203-210.
11. Crisona, N. J., and R. C. Strohman. 1983. Inhibition of contraction of cultured muscle fibers results in increased turnover of myofibrillar proteins but not of intermediate filament proteins. *J. Cell Biol.* 96:684-692.
12. Croop, J., and H. Holtzer. 1975. Response of myogenic and fibrogenic cells to cytochalasin-B and to colcemid. *J. Cell Biol.* 65:271-285.
13. Croop, J., Y. Toyama, A. A. Dlugosz, and H. Holtzer. 1980. Selective effects of phorbol 12-myristate 13-acetate on myofibrils and 10-nm filaments. *Proc. Natl. Acad. Sci. USA.* 77:5273-5277.
14. Croop, J., G. Dubyak, Y. Toyama, A. Dlugosz, A. Scarpa, and H. Holtzer. 1982. Effects of 12-O-tetradecanoyl-phorbol-13-acetate on myofibril integrity and Ca+2 content in developing myotubes. *Dev. Biol.* 89:460-474.
15. Delfiner, J. S., Y. Toyama, and H. Holtzer. 1978. Phagocytosis in myogenic cultures. *J. Cell Biol.* 79:370 a Abstr.
16. Dlugosz, A. A., S. J. Tapscott, and H. Holtzer. 1983. Effects of phorbol 12-myristate 13-acetate on the differentiation program of embryonic chick skeletal myoblasts. *Cancer Res.* 43:2780-2789.
17. Etlinger, J. D., and D. A. Fischman. 1973. M and Z band components and the assembly of myofibrils. *Cold Spring Harbor Symp. Quant. Biol.* 37:549-566.
18. Fallon, J. R., and V. T. Nachmias. 1980. Localization of cytoplasmic and skeletal myosins in developing muscle cells by double-label immunofluorescence. *J. Cell Biol.* 87:237-247.
19. Fellini, S., G. Bennett, and H. Holtzer. 1978. Selective binding of antibody against gizzard 10-nm filaments to different cell types in myogenic cultures. *Am. J. Anat.* 153:451-457.
20. Fischman, D. A. 1970. The synthesis and assembly of myofibrils in embryonic muscle. *In* Current Topics in Developmental Biology. A. Monroy and A. A. Moscona, editors. Academic Press, Inc., New York. 5:235-280.
21. Fischman, D. A. 1972. Development of striated muscle. *In* The Structure and Function of Muscle, 2nd edition, volume 1. G. H. Bourne, editor. Academic Press, New York. pp. 75-148.
22. Fuseler, J. W., and J. W. Shay. 1982. The association of desmin with the developing myofibrils of cultured embryonic rat heart myocytes. *Dev. Biol.* 91:448-457.
23. Gard, D., and E. Lazarides. 1980. The synthesis and distribution of desmin and vimentin during myogenesis in vitro. *Cell.* 19:263-275.
24. Glacy, S. D. 1983. Subcellular distribution of rhodamine-actin microinjected into living fibroblastic cells. *J. Cell Biol.* 97:1207-1213.
25. Gordon, D. J., Y. Yang, and E. D. Korn. 1976. Polymerization of *Acanthamoeba* actin. *J. Biol. Chem.* 251:7474-7479.
26. Gordon, W. E. 1978. Immunofluorescent and ultrastructural studies of "sarcomeric" units in stress fibers of cultured non-muscle cells. *Exp. Cell Res.* 117:253-260.
27. Gordon, W. E., and A. Bushnell. 1979. Immunofluorescent and ultrastructural studies of polygonal microfilament networks in respreading non-muscle cells. *Exp. Cell Res.* 120:335-348.
28. Gunning, P., P. Ponte, L. Kedes, R. J. Hickey, and A. I. Skoultchi. 1984. Expression of human cardiac actin in mouse L cells: a sarcomeric actin associated with a nonmuscle cytoskeleton. *Cell.* 36:709-715.
29. Harrington, W. F., M. Burke, and J. S. Barton. 1973. Association of myosin to form contractile systems. *Cold Spring Harbor Symp. Quant. Biol.* 37:77-85.
30. Heggeness, M. H., K. Wang, and S. J. Singer. 1977. Intracellular distributions of mechanochemical proteins in cultured fibroblasts. *Proc. Natl. Acad. Sci. USA.* 74:3883-

3887.
31. Holtzer, H., J. M. Marshall, and H. Finck. 1957. An analysis of myogenesis by the use of fluorescent antimyosin. *J. Biophys. Biochem. Cytol.* 3:705-723.
32. Holtzer, H. 1959. *In* Biological Organization Cellular and Subcellular. Proceedings of a symposium organized on behalf of UNESCO, held at the University of Edinburgh, Scotland; September, 1957. C. H. Waddington, editor. Pergamon Press, New York. pp. 142-152.
33. Holtzer, H. 1961. Aspects of chondrogenesis and myogenesis. *In* Molecular and Cellular Synthesis. 19th Growth Symposium. D. Rudnick, editor. The Ronald Press Company, New York. pp. 35-86.
34. Holtzer, H., and J. W. Sanger. 1972. Myogenesis: old views rethought. *In* Research in Muscle Development and the Muscle Spindle. B. Banker, R. Przybylski, and M. Victor, editors. Excerpta Medica, Amsterdam. pp. 122-133.
35. Holtzer, H., J. Sanger, H. Ishikawa, and K. Strahs. 1973. Selected topics in skeletal myogenesis. *Cold Spring Harbor Symp. Quant. Biol.* 37:549-566.
36. Holtzer, H., J. Croop, S. Dienstman, H. Ishikawa, and A. P. Somlyo. 1975. Effects of cytochalasin B and colcemide on myogenic cultures. *Proc. Natl. Acad. Sci. USA.* 72:513-517.
37. Holtzer, H., S. Fellini, N. Rubinstein, J. Chi, and K. Strahs. 1976. Cells, myosins, and 100-A filaments. *In* Cell Motility. R. Goldman, T. Pollard, and J. Rosenbaum, editors. Cold Spring Harbor, New York. pp. 823-839.
38. Holtzer, H., J. Croop, Y. Toyama, G. Bennett, S. Fellini, and C. West. 1980. Differences in differentiation programs between presumptive myoblasts and their daughters, the definitive myoblasts and myotubes. *In* Plasticity of Muscle. D. Pette, editor. Walter de Gruyter & Co., Berlin-New York, pp. 133-146.
39. Holtzer, H., G. S. Bennett, S. J. Tapscott, J. M. Croop, A. Dlugosz, and Y. Toyama. 1981. Changes in intermediate-sized filaments during myogenesis and neurogenesis. *In* International Cell Biology 1980-1981. H. G. Schweiger, editor. Springer-Verlag, Berlin. pp. 293-305.
40. Holtzer, H., J. Sasse, P. Antin, S. Tokunaka, M. Pacifici, A. Horwitz, and S. Holtzer. 1984. Lineages, DNA synthesis, postmitotic myoblasts and myofibrillogenesis. *Exp. Biol. Med.* 9:126-135.
41. Holtzer, H., S. Forry-Schaudies, P. Antin, G. Dubyak, and V. Nachmias. 1984. The tumor promoter TPA and the carcinogen EMS induce incoordinate synthesis of muscle proteins. *In* Gene Expression in Muscle. S. Wolf and R. Strohman, editors. Plenum Press, New York.
42. Holtzer, H., S. Forry-Schaudies, P. Antin, V. Nachmias, and G. Dubyak. 1985. Interactions between IFs, microtubules and myofibrils in fibrogenic and myogenic cells. *New York Acad. Sci.* In press.
43. Huxley, H. 1983. Molecular basis of contraction in cross-striated muscles and relevance to motile mechanisms in other cells. *In* Muscle and Nonmuscle Motility, Vol. 1. A. Stracher, editor. Academic Press, Inc., New York. pp. 1-104.
44. Ishikawa, H., R. Bischoff, and H. Holtzer. 1968. Mitosis and Intermediate-sized filament in developing muscle. *J. Cell Biol.* 38:538-551.
45. Korn, E. D. 1983. Actin polymerization and its regulation by proteins from non-muscle cells. *Physiol. Rev.* 62:672-737.
46. Kreis, T. E., and W. Birchmeier. 1980. Stress fiber sarcomeres of fibroblasts are contractile. *Cell.* 22:555-561.
47. Kreis, T. E., D. Geiger, and J. Schlessinger. 1982. Mobility of microinjected rhodamine actin within living chicken gizzard cells determined by fluorescence photobleaching recovery. *Cell.* 29:835-845.
48. Kuczmarski, E. R., and J. L. Rosenbaum. 1978. Chick brain actin and myosin. Isolation and characterization. *J. Cell Biol.* 80:341-355.
49. Lazarides, E. 1976. Actin, α-actinin, and tropomyosin interaction in the structural organization of actin filaments in nonmuscle cells. *J. Cell Biol.* 68:202-219.
50. Lazarides, E. 1980. Intermediate filaments as mechanical integrators of cellular space. *Nature (Lond.).* 283:249-256.
51. Manasek, F. J. 1968. Mitosis in developing cardiac muscle. *J. Cell Biol.* 37:191-196.
52. Menko, A. S., J. Croop, Y. Toyama, H. Holtzer, and D. Boettiger. 1982. The response of chicken embryo dermal fibroblasts to cytochalasin B is altered by Rous sarcoma virus-induced cell transformation. *Mol. Cell. Biol.* 2:320-330.
53. Nelson, W. J., and E. Lazarides. 1983. Switching of subunit composition of muscle spectrin during myogenesis in vitro. *Nature (Lond.).* 304:364-368.
54. Okazaki, K., and H. Holtzer. 1965. An analysis of myogenesis in vitro using fluorescein-labeled anti-myosin. *J. Cytochem. Histochem.* 13:726-739.
55. Pardo, J. V., J. D. Siliciano, and S. W. Craig. 1983. Vinculin is a component of an extensive network of myofibril-sarcolemma attachment regions in cardiac muscle fibers. *J. Cell Biol.* 97:1081-1088.
56. Peng, H. B., J. J. Wolosewick, and P.-C. Cheng. 1981. The development of myofibrils in cultured muscle cells: a whole-mount and thin-section electron microscopic study. *Dev. Biol.* 88:121-136.
57. Pollack, R., M. Osborn, and K. Weber. 1975. Patterns of organization of actin and myosin in normal and transformed cultured cells. *Proc. Natl. Acad. Sci. USA.* 72:994-998.
58. Pollard, T. D., and R. R. Weihing. 1974. Actin and myosin and cell movement. *CRC Crit. Rev. Biochem.* 2:1-65.
59. Rathke, P. C., M. Osborn, and K. Weber. 1979. Immunological and ultrastructural characterization of microfilament bundles: polygonal nets and stress fibers in an established cell line. *Eur. J. Cell Biol.* 19:40-48.
60. Sanger, J. W., J. M. Sanger, and B. M. Jockusch. 1983. Differences in the stress fibers between fibroblasts and epithelial cells. *J. Cell Biol.* 96:961-969.
61. Schliwa, M. 1981. Proteins associated with cytoplasmic actin. *Cell.* 25:587-590.
62. Small, J. V., G. Rinnerthaler, and H. Hinssen. 1982. Organization of actin meshworks in cultured cells: the leading edge. *Cold Spring Harbor Symp. Quant. Biol.* 46:599-611.
63. Sweeney, L. J., W. A. Clark, Jr., P. K. Umeda, R. Zak, and F. J. Manasek. 1984. Immunofluorescence analysis of the primordial myosin detectable in embryonic striated muscle. *Proc. Natl. Acad. Sci. USA.* 81:797-800.
64. Tapscott, S. J., G. S. Bennett, Y. Toyama, F. Kleinbart, and H. Holtzer. 1981. Intermediate filament proteins in the developing chick spinal cord. *Dev. Biol.* 86:40-54.
65. Tokuyasu, K. T. 1983. Visualization of longitudinally-oriented intermediate filaments in frozen sections of chicken cardiac muscle by a new staining method. *J. Cell Biol.* 97:562-565.
66. Vale, R. D., and E. M. Shooter. 1982. Alteration of binding properties and cytoskeletal attachment of nerve growth factor receptors in PC12 cells by wheat germ agglutinin. *J. Cell Biol.* 94:710-717.
67. Wang, E., and A. R. Taylor. 1976. Changes in microfilament organization and surface topography upon transformation of chick embryo fibroblasts with Rous sarcoma virus. *Proc. Natl. Acad. Sci. USA.* 73:4065-4059.

68. Weatherbee, J. A. 1981. Membranes and cell movement: interactions of membranes with the proteins of the cytoskeleton. *Int. Rev. Cytol., Suppl. 12.* pp. 113–176.

69. Weber, K., P. C. Rathke, M. Osborn, and W. W. Franke. 1976. Distribution of actin and tubulin in cells and in glycerinated cell models after treatment with cytochalasin B (CB). *Exp. Cell Res.* 102:285–297.

70. Wulf, E., A. Deboben, F. A. Bautz, H. Faulstich, and T. Wieland. 1979. Fluorescent phallotoxin, a tool for the visualizatin of cellular actin. *Proc. Natl. Acad. Sci. USA.* 76:4498–4502.

71. Zigmond, S. H., J. J. Otto, and J. Bryan. 1979. Organization of myosin in a submembranous sheath in well-spread human fibroblasts. *Exp. Cell Res.* 119:205–219.